arXiv:cond-mat/9904257v1 [cond-mat.str-el] 19 Apr 1999

Screening of a Point Charge: A Fixed-Node Diffusion Monte Carlo Study

Erik Koch[1], Olle Gunnarsson[1], and Richard M. Martin[2]

[1] Max-Planck-Institut für Festkörperforschung, 70569 Stuttgart, Germany
[2] Department of Physics and Materials Research Laboratory, University of Illinois, Urbana IL 61801, USA

Abstract. We study the static screening in a Hubbard-like model using fixed-node diffusion Monte Carlo. We find that the random phase approximation is surprisingly accurate even for metallic systems close to the Mott transition. As a specific application we discuss the implications of the efficient screening for the superconductivity in the doped Fullerenes. In the Monte Carlo calculations we use trial functions with two Gutzwiller-type parameters. To deal with such trial functions, we introduce a method for efficiently optimizing the Gutzwiller parameters, both in variational and in fixed-node diffusion Monte Carlo.

1 Introduction

The random phase approximation (RPA) is widely used throughout solid state physics. It properly describes the screening when the kinetic energy is much larger than the Coulomb energy. In the strongly correlated limit, however, it is qualitatively wrong. Little is known for the intermediate regime, where kinetic and Coulomb energy are comparable, and perturbative methods fail since there is no small parameter. In such a situation quantum Monte Carlo is the method of choice. Our goal is to investigate the screening in a strongly correlated system close to the Mott transition. To be specific we focus on the doped Fullerenes, like K_3C_{60}. These materials are strongly correlated and close to a Mott transition [1], but they are also superconductors with quite large transition temperatures ($T_c \approx 30\,\mathrm{K}$ for Rb_3C_{60}) [2]. The superconductivity is driven by the coupling to intramolecular phonons. These phonons mediate an effective electron–electron attraction which is, however, counteracted by the electron–electron repulsion, which is large in such strongly correlated systems. Unlike conventional superconductors, in the doped Fullerenes this repulsion is not reduced much by retardation effects. Therefore efficient screening is important for reducing the electron–electron repulsion sufficiently to allow for an electron–phonon driven superconductivity [3,4]. Using quantum Monte Carlo we find that even for quite strong correlations the RPA gives a surprisingly accurate description of the static screening on the metallic side of a Mott transition until the system is close to the transition [4]. Besides the immediate consequences this result has for our understanding of the superconductivity in the doped Fullerides, it should

also have quite general implications for the physics of systems close to a Mott transition.

We start by introducing the model Hamiltonian used to describe the doped Fullerenes. We briefly discuss the Löwdin downfolding technique that gives a general prescription for constructing low-energy Hamiltonians. Next we introduce the screening problem and discuss the results of the Monte Carlo calculations. Finally we review the quantum Monte Carlo methods used. We discuss the choice of the trial wave function and introduce a very efficient method for optimizing the Gutzwiller-type parameters.

2 Model Hamiltonian

Fullerites are crystals made of C_{60} molecules on an fcc lattice. They are characterized by very weak inter-molecular interactions. Therefore the discrete molecular levels merely broaden into narrow, well separated bands [5]. The valence band originates from the lowest unoccupied molecular orbital, which is a 3-fold degenerate t_{1u} orbital. In doped Fullerenes, there are alkali atoms sitting in the space between the C_{60} molecules. They do not affect the band structure around the Fermi energy very much. Only the filling of the t_{1u} band changes, since each alkali atom donates its valence electron. Hence for K_3C_{60} the (3-fold degenerate) t_{1u} band is half-filled. We are mainly interested in the properties of these valence-band electrons. To simplify the description we therefore want to get rid of the other bands. They can be projected out by the Löwdin downfolding technique [6]. The basic idea is to partition the Hilbert space into a subspace that contains the degrees of freedom that we are interested in (in our case the 't_{1u}-subspace') and the rest of the Hilbert space: $\mathcal{H} = \mathcal{H}_0 \oplus \mathcal{H}_1$. We can then write the Hamiltonian of the system as

$$H = \begin{pmatrix} H_{00} & H_{01} \\ H_{10} & H_{11} \end{pmatrix} , \tag{1}$$

where H_{ii} is the projection of the Hamiltonian onto subspace $\mathcal{H}_i$, while the H_{ij} $(i \neq j)$ contain the hybridization matrix elements between the two subspaces. Writing Green's function $G = (E - H)^{-1}$ in the same way, we can calculate the projection of G onto $\mathcal{H}_0$ [7]:

$$G_{00} = \Big(E - \underbrace{[H_{00} + H_{01}\,(E - H_{11})^{-1} H_{10}]}_{H_{\mathrm{eff}}(E)} \Big)^{-1} . \tag{2}$$

We see that the physics of the full system is described by an effective Hamiltonian $H_{\mathrm{eff}}(E)$ that operates on the subspace $\mathcal{H}_0$ only. We have, however, to pay a price for this drastic simplification: the effective Hamiltonian is energy dependent. In practice one approximates it with an energy-independent Hamiltonian $H_{\mathrm{eff}}(E_0)$. This works well if we are only interested in energies close to E_0. In solid C_{60} we have the fortunate situation that the bands retain the character of the molecular orbitals, since the hybridization matrix

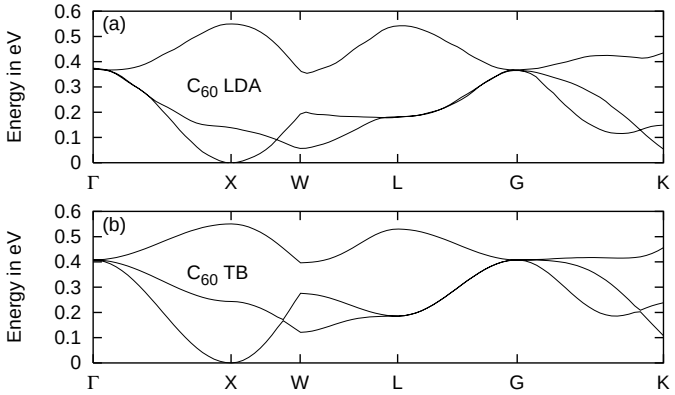

Fig. 1. Band structure (t_{1u} band) of solid C_{60} (fcc) (a) as calculated ab initio using the local density approximation [5] and (b) using a tight-binding Hamiltonian with only t_{1u} orbitals [8].

elements are small compared to the energy separations of the orbitals. In fact we can neglect the other bands altogether and get the hopping matrix elements $t_{in,\,jn'}$ between the t_{1u} orbitals n and n' on molecules i and j directly from a tight-binding parameterization [8,9]. To demonstrate how well this works, Fig. 1 shows the comparison of the ab initio t_{1u} band structure with the band structure obtained from the tight-binding Hamiltonian with only t_{1u} orbitals.

A realistic description of the electrons in the t_{1u} band also has to include the correlation effects which come from the Coulomb repulsion of electrons in t_{1u} orbitals on the same molecule. The resulting Hamiltonian which describes the interplay of the hopping of electrons and their Coulomb repulsion has the form

$$H = \sum_{\langle ij\rangle} \sum_{nn'\sigma} t_{in,jn'}\; c^{\dagger}_{in\sigma} c_{jn'\sigma} + \; U \sum_{i} \sum_{(n\sigma)<(n'\sigma')} n_{in\sigma} n_{in'\sigma'}. \tag{3}$$

The on-site Coulomb interaction U can be calculated within density functional theory [10]. It is given by the increase in the energy of the t_{1u} level per electron that is added to one molecule of the system. It is important to avoid double counting in the calculation of U. While the relaxation of the occupied orbitals and the polarization of neighboring molecules have to be included in the calculation, excitations within the t_{1u} band must be excluded, since they are contained explicitly in the Hamiltonian (3). The results are consistent with experimental estimates [11,12]: $U \approx 1.2 - 1.4\,\mathrm{eV}$. For comparison, the width of the t_{1u} band is in the range $W \approx 0.5 - 0.85\; eV$. To properly describe K_3C_{60} the effect of the orientational disorder [8,13] of the C_{60} molecules in the crystal are built into the hopping matrix elements $t_{in,jn'}$. Multiplet effects are not included, since they tend to be counteracted by the Jahn-Teller effect, which is also neglected.

In K_3C_{60} the system has three electrons per molecule. In the limit of weak correlations ($U = 0$), this corresponds to a metal with a half-filled conduction band. In the atomic limit ($U \to \infty$) the Coulomb energy dominates, forcing every molecule to be occupied by exactly three electrons, and suppressing any hopping. This is a Mott insulator. We therefore expect a metal-insulator transition for some finite value of the Coulomb interaction U. For the model Hamiltonian (3) with parameters describing K_3C_{60} it occurs for $U \approx 1.5 - 1.75\,\mathrm{eV}$ [1]. Given the estimates for the true value of U, K_3C_{60} is therefore close to the Mott transition, in a correlated metallic state.

3 Screening of a Point Charge

We now investigate how efficient the screening is in a strongly correlated system like K_3C_{60}. To be specific we analyze how a test charge q sitting on one molecule is screened by the conduction electrons in the t_{1u} band. To describe the influence of the test charge situated on the molecule at site c we include an additional term

$$H_q = q\,U \sum_{n\sigma} n_{cn\sigma} \tag{4}$$

in the Hamiltonian (3). Determining the electron density at site c for the system without test charge and for the system with a finite q we find the screening

$$\frac{\Delta n}{q} = \frac{n_c(0) - n_c(q)}{q}\,. \tag{5}$$

Let's first discuss the screening in the RPA. In the random phase approximation it only costs kinetic energy to screen the test charge. In the limit where a typical Coulomb integral U is large compared with the band width W, the kinetic energy cost of screening is relatively small compared with the potential energy gain. Therefore, within the random phase approximation, the screening is very efficient for large U. This means that as the test charge q is introduced, almost the same amount of electronic charge moves away from the site: $\Delta n \approx q$ for large U (see Fig. 2). The random phase approximation neglects, however, that when an electron leaves a site it has to find another site with a missing electron or there is an increase in Coulomb energy of the order of U. Thus the RPA is accurate for small values of U/W, while it is *qualitatively wrong* for large U/W. It is not clear what happens when Coulomb energy U and band width W are comparable.

To address this question we have performed quantum Monte Carlo calculations for the combined Hamiltonian

$$H = \sum_{\langle ij\rangle} \sum_{nn'\sigma} t_{in,jn'} c^\dagger_{in\sigma} c_{jn'\sigma} + U \sum_i \sum_{(n\sigma)<(n'\sigma')} n_{in\sigma} n_{in'\sigma'} + qU \sum_{n\sigma} n_{cn\sigma} \tag{6}$$

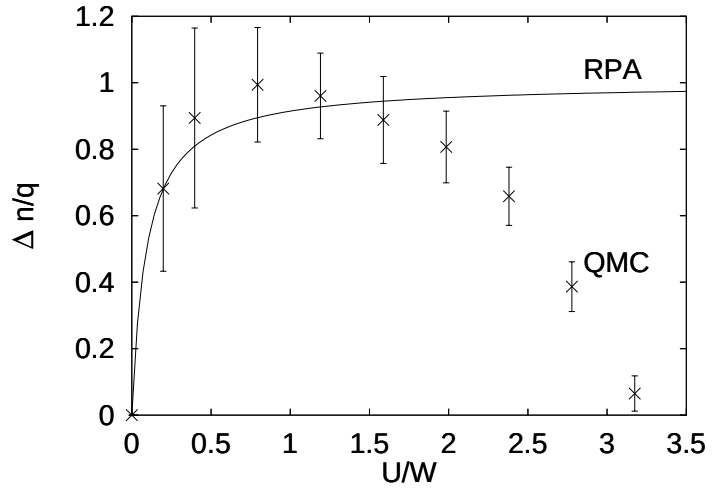

Fig. 2. Screening charge Δn on the site of the test charge ($q = 0.25\,e$) as a function of U/W, extrapolated to infinite cluster size. The full curve shows the screening charge in the RPA, obtained from Hartree calculations for the Hamiltonian (6). The crosses with errorbars give the results of the QMC calculations. The RPA screening remains rather accurate up to $U/W \sim 2$, but fails badly for larger values of U/W. The screening is very efficient for $U/W \sim 0.5 - 2.0$.

Since we are interested in the linear response, we should calculate the effect of an infinitesimally small test charge q. Because of the statistical error in a Monte Carlo calculation it is, however, difficult to determine the response to a small perturbation. To get a good signal-to-noise ratio, we would therefore like to use as large a test charge as possible. To estimate how large we can make q and still be in the linear response regime, we have performed Lanczos calculations for a small system of 4 molecules, where exact calculations are possible. Checking the response for different test charges we find that for $q \leq 0.25\,e$ the response is practically linear. The quantum Monte Carlo calculations were then performed for large clusters of $N_{\rm mol}$ =32, 48, 64, 72, and 108 molecules, corresponding to systems with 96, 144, 192, 216, and 324 electrons, and $q = 0.25$. To extrapolate the results $\Delta n(N_{\rm mol})$ to infinite systems size we used a finite-size scaling of the form $\Delta n = \Delta n(N_{\rm mol}) + \alpha/N_{\rm mol}$. The results are shown in Fig. 2. For rather small values of U/W ($\sim 0.5 - 1.0$), the RPA somewhat underestimates the screening. Such a behavior is also found in the electron gas [14]. For intermediate values of U/W ($\sim 1.0 - 2.0$) the RPA gives surprisingly accurate results. For larger U/W the screening rapidly breaks down, and the RPA becomes qualitatively wrong, as discussed above.

The efficient screening almost up to the Mott transition which occurs for $U/W \sim 2.5$ [1] has profound implications for the superconductivity in the

alkali doped Fullerenes. We will only give qualitative arguments here, a more detailed discussion can be found in [4]. In BCS theory the superconducting transition temperature is given by

$$T_c \propto e^{-1/(\lambda-\mu^*)} , \tag{7}$$

where $\lambda = N(0)\,V$ describes the electron–phonon coupling, which mediates the effective electron–electron attraction, $\mu^* = N(0)\,U^*$ is the Coulomb pseudopotential that describes the repulsive Coulomb interaction between electrons, and $N(0)$ is the density of states at the Fermi energy. Since the electrons couple to intramolecular phonons, the coupling constant V is to a good approximation a molecular property. Therefore increasing the density of states $N(0)$ will increase the electron–phonon coupling λ. This can be achieved by increasing the lattice constant of the solid Fullerene. Taking the C_{60} molecules further apart will decrease the hopping matrix elements $t_{in,jn'}$ thus narrowing the t_{1u} band and correspondingly increasing the density of states. If also U^* was a molecular quantity, i.e. independent of the lattice constant, and if $V > U^*$ which, of course, is the prerequisite for superconductivity, then according to (7) increasing the lattice constant would raise T_c. Such a variation of the transition temperature with the lattice constant is indeed found experimentally [2]. Here the variation of the lattice constant a is achieved by applying hydrostatic pressure (to reduce a) or by using 'larger' alkali metals like Rb and Cs to increase the lattice constant compared to K_3C_{60} (chemical pressure). This suggests that by inserting even more bulky ions or molecules, like NH_3, into the doped Fullerenes, could be increase T_c even further. As it turns out, however, T_c rapidly *decreases* with a when the lattice constant becomes too large, and eventually superconductivity disappears. This drop in T_c can be understood as a natural consequence of the breakdown of the screening close to the Mott transition. In the doped Fullerenes U^* is essentially given by $U\,(1 - \Delta n/q)$, where U is the unscreened Coulomb matrix element (cf. the interaction term in the Hamiltonian) and $\Delta n/q$ describes the screening by the t_{1u} electrons. U is practically independent of the lattice constant, while the screening efficiency changes with the band width as shown in Fig. 2. For U/W in the region $1.0 - 2.0$ the screening is almost RPA-like and does not vary very much, which means that in this region U^* is almost independent of the lattice constant a. In this region T_c thus increases with a. For even smaller band width, or correspondingly larger lattice constants, the screening rapidly becomes inefficient. Now U^* increases with the lattice constant, leading to a decrease of $\lambda - \mu^*$. Hence for a too large, T_c rapidly decreases with a and eventually vanishes. Since the screening only breaks down close to the metal-insulator transition, we have the interesting situation that *T_c peaks close to a Mott transition!*

The efficient screening found in the Monte Carlo calculations also explains why the coupling to the alkali-phonons is weak. Each C_{60} molecule is surrounded by 14 alkali ions with very weak force constants. When an electron arrives on a molecule one would therefore expect that the surrounding alkali

ions respond strongly. This was, however, not confirmed by experiment [15]. That result can be naturally understood as an effect of the efficient screening: When an electron arrives on a molecule other electrons leave, effectively leaving the molecule almost neutral. The alkali ions then only see a small change in the net charge and therefore respond weakly, leading to a small electron–phonon coupling. But being molecular crystals, doped Fullerenes also have intramolecular phonons. Some of those intramolecular phonons shift the t_{1u} levels in such a way that the center of gravity of the energy levels is not changed. These are the modes that are not screened by the transfer of charged. They are therefore the modes that drive superconductivity in the Fullerides.

4 Quantum Monte Carlo

We now turn to the question of how the results shown in Fig. 2 were obtained. To keep the notation simple we will discuss the different methods for a simple Hubbard model (only one orbital per site, next neighbor hopping matrix elements $t_{ij} = -t$):

$$H = -t \sum c_i^\dagger c_j + U \sum n_{i\uparrow} n_{i\downarrow} \; . \tag{8}$$

The generalization to Hamiltonians like (3) is straightforward.

The first step in the quantum Monte Carlo approach is to identify a trial function Ψ_T. For the Hubbard model that function should balance the opposing tendencies of the hopping term and the interaction: Without interaction (i.e. for $U = 0$) the ground state of the Hamiltonian (8) is the Slater determinant Φ that maximizes the kinetic energy. Without hopping ($t = 0$) the interaction is minimized. Since only doubly occupied sites, i.e. sites with $n_{i\uparrow} = 1$ and $n_{i\downarrow} = 1$, contribute to the Coulomb energy, the electrons are distributed as uniformly as possible over the lattice to minimize the number of double occupancies. A good compromise between these two extremes is to start from the non-interacting wavefunction Φ but reduce the weight of configurations R with large double occupancies $D(R)$. This leads (up to normalization) to the Gutzwiller wavefunction [16]:

$$\Psi_T(R) = g^{D(R)} \, \Phi(R), \tag{9}$$

with $g \in (0, 1]$ the Gutzwiller parameter. In configuration space the Coulomb term in the Hamiltonian is given by $U\, D(R)$. Thus the Gutzwiller factor reflects the interaction term in the Hubbard Hamiltonian. In this spirit we can also construct trial functions for Hamiltonians with additional terms like the screening Hamiltonian (6). We add a second Gutzwiller factor that reflects the interaction with the test charge $q\, U\, n_c(R)$:

$$\Psi_T(R) = g^{D(R)} \, h^{n_c(R)} \, \Phi(R) \; . \tag{10}$$

Changing the additional Gutzwiller factor h we can vary the occupation of the site with the test charge.

4.1 Variational Monte Carlo

Since the Gutzwiller factor, like the interaction term, is diagonal in configuration space, we have to perform a sum over all configurations R in order to calculate the energy expectation value for a Gutzwiller wavefunction:

$$E_T = \frac{\langle\Psi_T|H|\Psi_T\rangle}{\langle\Psi_T|\Psi_T\rangle} = \frac{\sum_R E_{\rm loc}(R)\,\Psi_T^2(R)}{\sum_R \Psi_T^2(R)}\,, \tag{11}$$

where we have introduced the local energy for a configuration R

$$E_{\rm loc}(R) = \sum_{R'} \frac{\langle\Psi_T|R'\rangle\,\langle R'|H|R\rangle}{\langle\Psi_T|R\rangle} = \sum_{R'}{}' \; t\,\frac{\Psi_T(R')}{\Psi_T(R)} + U\,D(R)\,. \tag{12}$$

Since the number of configurations R grows exponentially with system-size, the summations in (11) can only be done explicitly for very small systems. For larger problems we use variational Monte Carlo [17]. The idea is to perform a random walk in the space of configurations, with transition probabilities $p(R \to R')$ chosen such that the configurations $R_{\rm VMC}$ in the random walk have the probability distribution function $\Psi_T^2(R)$. Then

$$E_{\rm VMC} = \frac{\sum_{R_{\rm VMC}} E_{\rm loc}(R_{\rm VMC})}{\sum_{R_{\rm VMC}} 1} \approx \frac{\sum_R E_{\rm loc}(R)\,\Psi_T^2(R)}{\sum_R \Psi_T^2(R)} = E_T. \tag{13}$$

The transition probabilities can be determined from detailed balance

$$\Psi_T^2(R)\,p(R \to R') = \Psi_T^2(R')\,p(R' \to R) \tag{14}$$

which is fulfilled by the choice $p(R \to R') = 1/N \;\; \min[1, \Psi_T^2(R')/\Psi_T^2(R)]$, with N being the maximum number of possible transitions. It is sufficient to consider only transitions between configurations that are connected by the Hamiltonian, i.e. transitions in which one electron hops to a neighboring site. The standard prescription is then to propose a transition $R \to R'$ with probability $1/N$ and accept it with probability $\min[1, \Psi_T^2(R')/\Psi_T^2(R)]$. This works well for U not too large. For strongly correlated systems, however, the random walk will stay for long times in configurations with a small number of double occupancies $D(R)$, since most of the proposed moves will increase D and hence be rejected with probability $\approx 1 - g^{D(R')-D(R)}$.

There is, however, a way to integrate-out the time the walk stays in a given configuration. To see how, we first observe that for the local energy (12) the ratio of the wavefunctions for all transitions induced by the Hamiltonian have to be calculated. This in turn means that we also know all transition probabilities $p(R \to R')$. We can therefore eliminate any rejection (i.e. accept with probability one) by proposing moves with probabilities

$$\tilde{p}(R \to R') = \frac{p(R \to R')}{\sum_{R'} p(R \to R')} = \frac{p(R \to R')}{1 - p_{\rm stay}(R)}\,. \tag{15}$$

Checking detailed balance (14) we find that now we are sampling configurations $\tilde{R}_{\mathrm{VMC}}$ from the probability distribution function $\Psi_T^2(R)\,(1-p_{\mathrm{stay}}(R))$. To compensate for this we assign a weight $w(R) = 1/(1-p_{\mathrm{stay}}(R))$ to each configuration R. The energy expectation value is then given by

$$E_T \approx \frac{\sum_{\tilde{R}_{\mathrm{VMC}}} w(\tilde{R}_{\mathrm{VMC}})\, E_{\mathrm{loc}}(\tilde{R}_{\mathrm{VMC}})}{\sum_{\tilde{R}_{\mathrm{VMC}}} w(\tilde{R}_{\mathrm{VMC}})}\ . \tag{16}$$

The above method is quite efficient since it ensures that in every Monte Carlo step a new configuration is created. Instead of staying in a configuration where Ψ_T is large, this configuration is weighted with the expectation value of the number of steps the simple Metropolis algorithm would stay there. This is particularly convenient for simulations of systems with strong correlations: Instead of having to do longer and longer runs as U is increased, the above method produces, for a fixed number of Monte Carlo steps, results with comparable error estimates.

Correlated sampling So far we have only specified the form of the trial function Ψ_T. The goal of a variational calculation is now to identify the parameters that result in the best trial function. A criterion for a good trial function is e.g. a low variational energy. To find the wavefunction that minimizes the variational energy we could perform independent VMC calculations for a set of different trial functions. It is, however, difficult to compare the energies from these calculations since each VMC result comes with its own statistical errors. This problem can be avoided with correlated sampling [18]. The idea is to use the same random walk for calculating the expectation value of all the different trial functions. This reduces the *relative* errors and hence makes it easier to find the minimum.

Let us assume we have generated a random walk R_{VMC} using Ψ_T as the trial function. Using the same random walk, we can then estimate the energy expectation value (13) for a different trial function $\tilde{\Psi}_T$, by introducing the reweighting factors $\tilde{\Psi}_T^2(R)/\Psi_T^2(R)$:

$$\tilde{E}_T \approx \frac{\sum_{R_{\mathrm{VMC}}} \tilde{E}_{\mathrm{loc}}(R)\, \tilde{\Psi}_T^2(R)/\Psi_T^2(R)}{\sum_{R_{\mathrm{VMC}}} \tilde{\Psi}_T^2(R)/\Psi_T^2(R)}\ . \tag{17}$$

with

$$\begin{aligned}\tilde{E}_{\mathrm{loc}}(R) &= \sum_{R'} t\frac{\tilde{\Psi}_T(R')}{\tilde{\Psi}(R)} + U\ D(R) \\ &= \sum_{R'} t\frac{\Psi_T(R')}{\Psi_T(R)}\ \frac{\tilde{\Psi}_T(R')/\Psi_T(R')}{\tilde{\Psi}_T(R)/\Psi_T(R)} + U\ D(R)\end{aligned} \tag{18}$$

We notice that (also in $\tilde{E}_{\mathrm{loc}}$) the new trial function $\tilde{\Psi}_T$ appears only in ratios with the old Ψ_T. For trial functions (9) that differ only in the Gutzwiller

factor this means that the Slater determinants cancel, leaving only powers $(\tilde{g}/g)^{D(R)}$. Since $D(R)$ is *integer* we can then rearrange the sums in (17) into polynomials in $\tilde{g}/g$. To find the optimal Gutzwiller parameter we then pick a reasonable g, perform a VMC run for $\Psi_T(g)$ during which we also estimate the coefficients for these polynomials. We can then calculate $E(\tilde{g})$ by simply evaluating the ratio of the polynomials. Since there are typically only of the order of some ten non-vanishing coefficients this method is very efficient.

The idea of rewriting the sum over configurations into a polynomial can be easily generalized to trial functions with more correlation factors of the type $r^{c(R)}$, as long as the correlation function $c(R)$ is integer-valued on the space of configurations. As a specific example of how the method works in practice, Fig. 3 shows the result of a correlated sampling run for the trial function (10).

4.2 Fixed-node diffusion Monte Carlo

Diffusion Monte Carlo [19] allows us, in principle, to sample the true ground state of a Hamiltonian. The basic idea is to use a projection operator that has the lowest eigenstate as a fixed point. For a lattice problem where the spectrum is bounded $E_n \in [E_0, E_{\max}]$, the projection is given by

$$|\Psi^{(n+1)}\rangle = [1 - \tau(H - E_0)]\, |\Psi^{(n)}\rangle\,; \quad |\Psi^{(0)}\rangle = |\Psi_T\rangle. \tag{19}$$

If $\tau < 2/(E_{\max} - E_0)$ and $|\Psi_T\rangle$ has a non-vanishing overlap with the ground state, the above iteration converges to $|\Psi_0\rangle$. There is no time-step error involved. Because of the prohibitively large dimension of the many-body Hilbert space, the matrix-vector product in (19) cannot be done exactly. Instead, we rewrite the equation in configuration space

$$\sum |R'\rangle\langle R'|\Psi^{(n+1)}\rangle = \sum_{R,R'} |R'\rangle \underbrace{\langle R'|1 - \tau(H - E_0)|R\rangle}_{=:F(R',R)} \langle R|\Psi^{(n)}\rangle \tag{20}$$

and perform the propagation in a stochastic sense: $\Psi^{(n)}$ is represented by an ensemble of configurations R with weights $w(R)$. The transition matrix element $F(R', R)$ is rewritten as a transition probability $p(R \to R')$ times a normalization factor $m(R', R)$. The iteration (20) is then stochastically performed as follows: For each R we pick a new configuration R' with probability $p(R \to R')$ and multiply its weight by $m(R', R)$. Then the new ensemble of configurations R' with their respective weights represents $\Psi^{(n+1)}$. Importance sampling decisively improves the efficiency of this process by replacing $F(R', R)$ with $G(R', R) = \langle \Psi_T|R'\rangle\, F(R', R)/\langle R|\Psi_T\rangle$, so that transitions from configurations where the trial function is small to configurations with large trial function are enhanced:

$$\sum |R'\rangle\langle \Psi_T|R'\rangle\langle R'|\Psi^{(n+1)}\rangle = \sum_{R,R'} |R'\rangle\, G(R', R)\, \langle \Psi_T|R\rangle\, \langle R|\Psi^{(n)}\rangle. \tag{21}$$

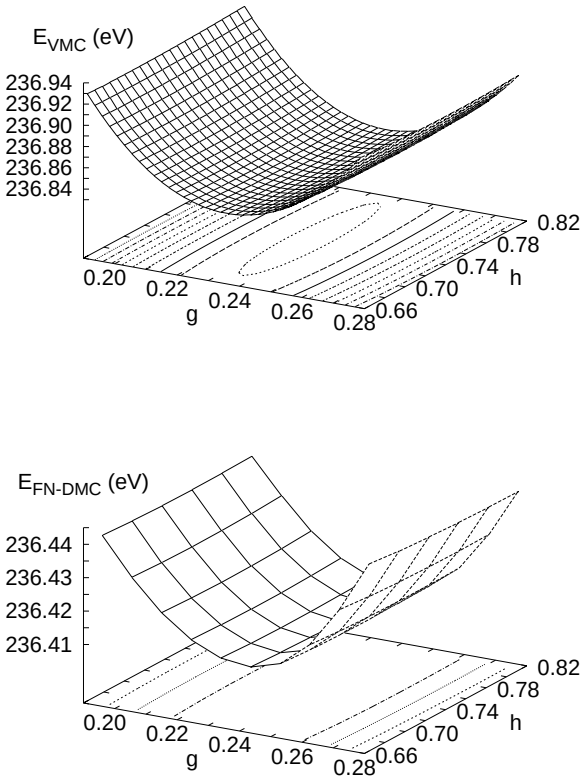

Fig. 3. Correlated sampling for the parameters g and h in the generalized Gutzwiller wavefunction $|\Psi_T\rangle = g^D h^{n_c} |\Phi\rangle$, cf. eqn. (10), in variational (upper plot) and fixed-node diffusion Monte Carlo (lower plot). The plots show the energy as a function of the Gutzwiller parameters g and h, both as surfaces and contours. The calculations were done for an fcc cluster of 64 molecules with 96+96 electrons (half-filled t_{1u}-band), an on-site Hubbard interaction $U = 1.25\,\mathrm{eV}$, and a test charge of $q = 1/4\,\mathrm{e}$.

Now the ensemble of configurations represents the product $\Psi_T\,\Psi^{(n)}$. After a large number n of iterations the ground state energy is then given by the mixed estimator

$$E_0 = \frac{\langle\Psi_T|H|\Psi^{(n)}\rangle}{\langle\Psi_T|\Psi^{(n)}\rangle} \approx \frac{\sum_R E_{\mathrm{loc}}(R)\; w(R)}{\sum_R w(R)}. \tag{22}$$

As long as the evolution operator has only non-negative matrix elements $G(R', R)$, all weights $w(R)$ will be positive. If, however, G has negative matrix

elements there will be both configurations with positive and negative weight. Their contributions to the estimator (22) tend to cancel so that eventually the statistical error dominates, rendering the simulation useless. This is the infamous sign problem. A straightforward way to get rid of the sign problem is to remove the offending matrix elements from the Hamiltonian, thus defining a new Hamiltonian H_{eff} by

$$\langle R'|H_{\text{eff}}|R\rangle = \begin{cases} 0 & \text{if } G(R',R) < 0 \\ \langle R'|H|R\rangle & \text{else} \end{cases} \tag{23}$$

For each off-diagonal element $\langle R'|H|R\rangle$ that has been removed, a term is added to the diagonal:

$$\langle R|H_{\text{eff}}|R\rangle = \langle R|H|R\rangle + \sum_{R'} \Psi_T(R')\langle R'|H|R\rangle/\Psi_T(R). \tag{24}$$

This is the fixed-node approximation for lattice Hamiltonians [20]. H_{eff} is by construction free of the sign problem and variational, i.e. $E_0^{\text{eff}} \geq E_0$. The equality holds if $\Psi_T(R')/\Psi_T(R) = \Psi_0(R')/\Psi_0(R)$ for all R, R' for which $G(R',R)$ is negative.

Fixed-node diffusion Monte Carlo for a lattice Hamiltonian thus means that we choose a trial function from which we construct an effective Hamiltonian and determine its ground state by diffusion Monte Carlo. Because of the variational property, we want to pick the Ψ_T such that E_0^{eff} is minimized, i.e. we want to optimize the trial function, or, equivalently, the effective Hamiltonian. Also here we can use the concept of correlated sampling. For optimizing the Gutzwiller parameter g we can even exploit the idea of rewriting the correlated sampling sums into polynomials in $\tilde{g}/g$, that we already have introduced in VMC. There is, however, a problem arising from the fact that the weight of a given configuration $R^{(n)}$ in iteration n is given by the product $w(R^{(n)}) = \prod_{i=1}^{n} m(R^{(i)}, R^{(i-1)})$. Each individual normalization factor $m(R',R)$ can be written as a finite polynomial, but the order of the polynomial for $w(R^{(n)})$ increases steadily with the number of iterations. It is therefore not practical to try to calculate the ever increasing number of coefficients for the correlated sampling function $E^{(n)}(\tilde{g})$. But since we still can easily calculate the coefficients for the $m(R',R)$, we may use them to evaluate $E^{(n)}(\tilde{g})$ in each iteration on a set of predefined values $\tilde{g}_i$ of the Gutzwiller parameter. Figure 3 shows an example, again for the more general trial function (10).

Extrapolated estimator So far we have only considered estimators for the total energy. For determining the screening, however, we need to know the charge density n_c on site c. It is no problem to calculate the expectation value $n_c(\text{VMC}) = \langle\Psi_T|\hat{n}_c|\Psi_T\rangle$ in variational Monte Carlo. Diffusion Monte Carlo gives, however, only the mixed estimator $n_c(\text{DMC}) = \langle\Psi_T|\hat{n}_c|\Psi_0\rangle$. Since the density operator does not commute with the Hamiltonian, the mixed

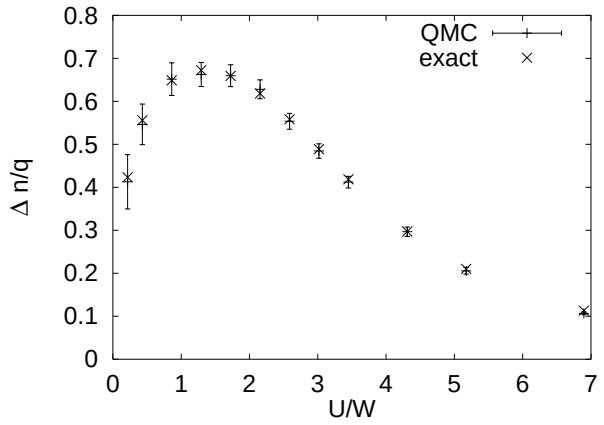

Fig. 4. Screening charge Δn on the site of the test charge ($q = 0.25\,\mathrm{e}$) as a function of U/W, where U is the Coulomb interaction and W is the band width. Exact diagonalization and QMC calculations have been performed for four molecules (12 electrons). The figure shows that the QMC calculations are quite accurate over the whole range of U/W.

estimator is different from expectation $n_c(\mathrm{QMC}) = \langle\Psi_0|\hat{n}_c|\Psi_0\rangle$. For a good choice of the trial function the true expectation value can be determined using the extrapolated estimator $n_c(\mathrm{QMC}) \approx 2\, n_c(\mathrm{DMC}) - n_c(\mathrm{VMC})$.

To test the accuracy of this approach to the screening problem, which besides the extrapolated estimator also involves the fixed-node approximation, we have compared the results of the quantum Monte Carlo calculations with the exact results from exact diagonalization for a small system of four molecules (12 electrons). As illustrated by Fig. 4, the QMC calculations for determining the screening charge are very accurate.

Acknowledgment. This work has been supported by the Alexander-von-Humboldt-Stiftung under the Feodor-Lynen-Program and the Max-Planck-Forschungspreis, and by grant No. DEFG02-96ER45439 from the Department of Energy.

References

1. Gunnarsson, O., Koch, E., and Martin, R.M. (1996) Mott transition in degenerate Hubbard models: Application to doped Fullerenes, *Phys. Rev. B* **54**, R11026
2. Gunnarsson, O. (1997) Superconductivity in Fullerides, *Rev. Mod. Phys.* **69**, 575-606
3. Gunnarsson, O., Zwicknagl, G. (1992) Coulomb Pseudopotential, Screening and Superconductivity in C_{60}, *Phys. Rev. Lett.* **69**, 957-960 ; Gunnarsson, O.,

Rainer, D., Zwicknagl, G. (1992) Screened interaction and Coulomb pseudopotential in C_{60}, *Int. J. Mod. Phys.* **6**, 3993-4005
4. Koch, E., Gunnarsson, O., Martin, R.M. (1999) Screening, Coulomb pseudopotential, and superconductivity in alkali-doped Fullerenes, *preprint* , `cond-mat/9902241`
5. Erwin, S. C. (1993) Electronic Structure of the Alkali-Intercalated Fullerides, Endohedral Fullerenes, and Metal-Adsorbed Fullerenes, in W. E. Billups and M. A. Ciufolini (Eds.), *Buckminsterfullerenes*, VCH Publishers, New York, pp. 217-253
6. Löwdin, P. O. (1951) A Note on the Quantum-Mechanical Perturbation Theory, *J. Chem. Phys.* **19**, 1396-1401
7. see e.g. Inversion by Partitioning, in W. H. Press, B. P. Flannery, S. A. Teukolsky, and W. T. Vetterling, *Numerical Recipes in Fortran: The Art of Scientific Computing*, Cambridge University Press, 1992, p. 70
8. Gunnarsson, O., Satpathy, S., Jepsen, O., and Andersen, O. K. (1991) Orientation of C_{60} Clusters in Solids, *Phys. Rev. Lett.* **67**, 3002 ; Satpathy, S., Antropov, V. P., Andersen, O. K., Jepsen, O., Gunnarsson, O., and Liechtenstein, A. I. (1992) Conduction-band structure of alkali-metal-doped C_{60}, *Phys. Rev. B* **46**, 1773
9. Gunnarsson, O., Erwin, S. C., Koch, E., and Martin, R. M. (1998) Role of alkali atoms in A_4C_{60}, *Phys. Rev. B* **57**, 2159
10. Antropov, V. P., Gunnarsson, O., and Jepsen, O. (1992) Coulomb integrals and model Hamiltonians for C_{60}, *Phys. Rev. B* **46**, 13647
11. Brühwiler, P. A., Maxwell, A. J., Nilsson, A., Mårtensson, N., and Gunnarsson, O. (1993) Auger and photoelectron study of the Hubbard U in C_{60}, K_3C_{60}, and K_6C_{60}, *Phys. Rev. B* **48**, 18296
12. Lof, R. W., van Veenendaal, M. A., Koopmans, B., Jonkman, H. T. and Sawatzky, G. A. (1992) Band Gap, Excitons, and Coulomb interaction in solid C_{60}, *Phys. Rev. Lett.* **68**, 3924
13. Mazin, I.I., Rashkeev, S.N., Antropov, V.P., Jepsen, O., Liechtenstein, A.I., and Andersen O.K. (1992) Quantitative theory of superconductivity in doped C_{60}, *Phys. Rev. B* **45**, 5114
14. Hedin, L., and Lundqvist, S. (1969) Effects of Electron-Electron and Electron-Phonon Interactions on the One-Electron States of Solids, in H. Ehrenreich, D. Turnbull and F. Seitz (Eds.), *Solid State Physics*, **23**, Academic Press, New York, pp. 1-181 ; Moroni, S., Ceperley, D.M., and Senatore, G. (1995) Static Response and Local Field Factor of the Electron Gas, *Phys. Rev. Lett.* **75**, 689
15. Ebbesen, T.W., Tsai, J.S., Tanigaki, K., Hiura, H., Shimakawa, Y., Kubo, Y., Hirosawa, I., Mizuki, J. (1992) , *Physica C* **203**, 163; Burk, B., Crespi, V.H., Zettl, A., Cohen, M.L. (1994) , *Phys. Rev. Lett.* **72**, 3706
16. Gutzwiller, M. C. (1963) Effect of correlation on the ferromagnetism of transition metals, *Phys. Rev. Lett.* **10**, 159
17. Horsch, P. and Kaplan, T. A. (1983) Exact and Monte Carlo studies of Gutzwiller's state for the localised-electron limit in one dimension, *J. Phys. C* **16**, L1203; Metropolis, N., Rosenbluth, A. W., Rosenbluth, N. M., Teller, A. H., and Teller, E. (1953) Equation of State Calculations by Fast Computing Machines, *J. Chem. Phys.* **21**, 1087
18. Ceperley, D. M., Chester, G. V., and Kalos, M. H. (1977) Monte Carlo simulation of a many-Fermion study, *Phys. Rev. B* **16**, 3081; Umrigar, C. J., Wilson,

K. G., and Wilkins, J. W. (1988) Optimized Trial Wave Functions for Quantum Monte Carlo Calculations, *Phys. Rev. Lett.* **60**, 1719 Koch, E., Gunnarsson, O., and Martin, R.M (1999) Optimization of Gutzwiller Wavefunctions in Quantum Monte Carlo, *preprint* , `cond-mat/9903070`

19. Trivedi, N. and Ceperley, D. M. (1989) Green-function Monte Carlo study of quantum antiferromagnets, *Phys. Rev. B* **40**, 2737
20. ten Haaf, D. F. B., van Bemmel, H. J. M., van Leeuwen, J. M. J., and van Saarloos, W. (1994) Fixed-node quantum Monte Carlo method for lattice Fermions, *Phys. Rev. Lett.* **72**, 2442; ten Haaf, D. F. B., van Bemmel, H. J. M., van Leeuwen, J. M. J., van Saarloos, W. and Ceperley, D. M. (1995) Proof for an upper bound in fixed-node Monte Carlo for lattice Fermions, *Phys. Rev. B* **51**, 13039 Calandra, M., Sorella, S. (1998) Numerical study of the two-dimensional Heisenberg model using a Green function Monte Carlo technique with a fixed number of walkers, *Phys. Rev. B* **57**, 11446 ; Cosentini, A.C., Capone, M., Guidoni, L., and Bachelet, G.B. (1998) Phase separation in the 2D Hubbard model: a fixed-node quantum Monte Carlo study, *Phys. Rev. B* **58**, R14685